

Calorimetric and powder X-ray diffraction studies on dissociation of methane hydrate in porous media

Akihiro Hachikubo^{1,*}, Satoshi Takeya², Evgeny Chuvilin³, Vladimir Istomin⁴

¹Kitami Institute of Technology, Kitami 090-8507, Japan, ²National Institute of Advanced Industrial Science and Technology (AIST), Tsukuba 305-8565, Japan, ³Gazprom VNIIGAZ LLC, Moscow Region, 142717, Russia, ⁴Moscow State University, Moscow 119991, Russia

* Corresponding author. E-mail: hachi@mail.kitami-it.ac.jp

Dissociation processes of synthetic methane hydrate with glass beads were reported by using a calorimetric system and powder X-ray diffraction. Methane hydrate formed with coarse glass beads (size: 30.8, 56.3, and 100.4 μm) rather quickly dissociated at 150-200 K, whereas about 40 % of that with fine glass beads (size: 0.4 μm) still survived at 200 K. These results are contrasting with the size effect of methane hydrate particles reported by Takeya *et al.* (2005) that larger particles can retain themselves than smaller particles.

1. INTRODUCTION

Gas hydrates are guest-host compounds and are crystalline materials consisting of water molecules that include guest molecules inside hydrogen-bonded water cages. Natural gas hydrates exist under the conditions of low temperature and high partial pressure of guest gases, as they exist in the sea/lake bottom sediments and permafrost layers. They are expected as a possible global source of energy^{1,2} and also concerned as a large reservoir of methane which may cause the global warming by their dissociation.

It is known that some gas hydrates can be stored at the atmospheric pressure just below the melting point of ice (273.2 K) even though this is well outside the zone of thermodynamic stability of the hydrate^{3,4}, an effect that has been termed "self-preservation"^{5,6}. A comprehensive understanding of the preservation of methane hydrate is important for the understanding of hydrate-related climate change in the earth. Until recently, the phenomena have been studied and its mechanism is being solved from a physicochemical point of view⁷⁻¹¹. However, not many studies on gas hydrate stability under natural settings have been performed^{5,12}.

Effect of porous materials with different sizes (submicron to 100 micron) on the dissociation process for pore methane hydrate accumulation was

examined by using calorimeter and powder X-ray diffraction (PXRD). Powder diffraction technique has been widely used to measure dissociation process of gas hydrates so far^{11,13-15}. In this study, we additionally apply calorimeter for the measurements of hydrate dissociation. The calorimetry is available to detect both solid water (ice) and liquid water being formed due to hydrate dissociations. The rate-determining steps for methane hydrate dissociation within macro pore are also discussed.

2. MATERIALS AND METHODS

2.1. Sample preparation

Methane hydrate samples in porous media were formed from ice-glass beads mixture. The spherical glass beads with four different size were used for hydrate sample preparations; COSMO55 (JGC C&C Ltd.), GBL-30 and GBL-60 (The Association of Powder Process Industry and Engineering, Japan), and SPL-100 (Union Co., Ltd.). The distributions of grain size were measured using a laser diffraction particle size analyzer (SALD-2100, Shimadzu Corporation). The grain size distribution and their images by FE-SEM (JSM-7400F, JEOL Ltd.) are shown in Fig. 1.

About 1 g of fine ice powder (mean grain size: less than 0.05 mm) and 5 g of glass beads were mixed in a small pressure cell (volume: 20 mL) at 255 K. The cell was evacuated and kept the temperature at 274.2 K for several hours to melt the ice. Research-grade

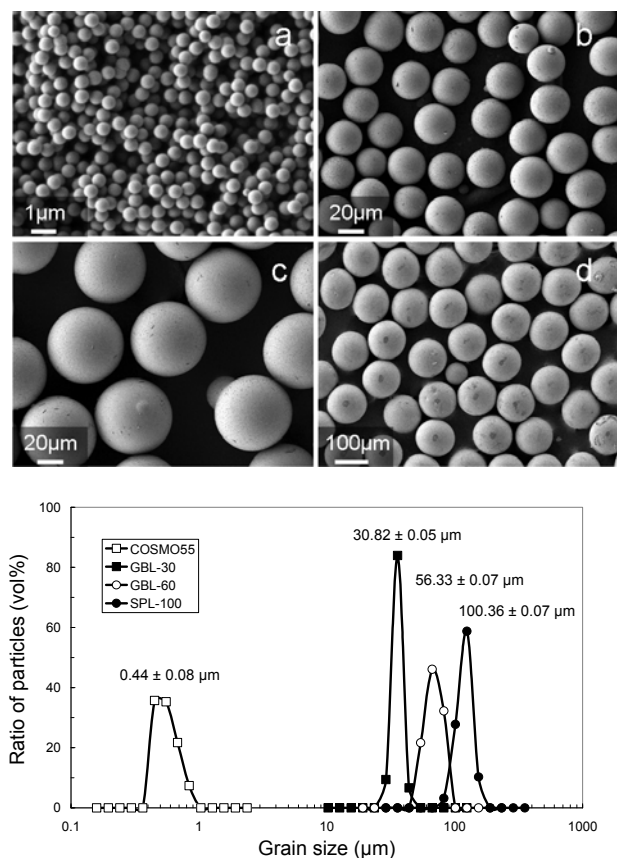


Figure 1. FE-SEM images of glass beads, size distributions, mean diameters and their standard deviations. (a) COSMO55, (b) GBL-30, (c) GBL-60, (d) SPL-100.

methane (99.99% purity) supplied by Takachiho Chemical Industry was pressurized at 5 MPa for more than 1.5 days to form methane hydrate. After confirmation of no significant pressure decrease (less than $0.01 \text{ MPa hour}^{-1}$) the sample was retrieved from the cell at the temperature of liquid nitrogen. These hydrate samples were used for the hydrate dissociation measurements by means of calorimeter and PXRD.

To assess the effect of glass beads for cage occupancy of methane, Raman spectroscopic measurements were also performed. Raman spectra of the samples were obtained with a spectrometer (RMP-210; JASCO Corporation) using a green laser (emitting a 532 nm line and providing 100 mW at the sample) as an excitation source. The spectrometer has a single-dispersed monochromator system equipped with $1800 \text{ grooves mm}^{-1}$ holographic diffraction grating device and thermoelectrically cooled CCD detector. The

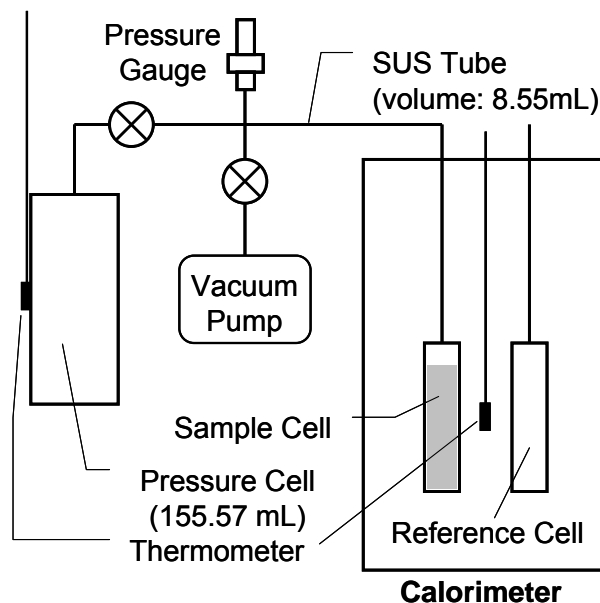


Figure 2. Schematic view of the calorimetric system.

measurements were performed in the range 2800 to 3000 cm^{-1} to check the C-H stretching peaks of methane at 123 K. Cage occupancies of these different size cages and hydration numbers were estimated using the statistical thermodynamic model^{16,17}.

2.2. Calorimetric measurement

The experimental setup for calorimetry was similar to that used in the previous study¹⁸⁻²⁰. Calorimetric system is shown in Fig. 2. About 2.7 g of the samples were set into a small pressure cell (volume: 3.7 mL) specially designed for the Tian-Calvet type heat-flow calorimeter (BT2.15, Setaram Instrumentation) and their dissociation process was monitored. The reference cell filled with pure nitrogen was introduced to the calorimeter against room temperature fluctuations.

The sample cell was set into the calorimeter at 93 K and connected with the other pressure cell (volume: 155.57 mL) for a smooth dissociation of the hydrate sample and an expansion of dissociated gas^{3,18}. The total volume of the system was enough to keep under the atmospheric pressure even after hydrate dissociation. The internal pressure was monitored by a pressure gauge (AP-10S, KEYENCE Corporation) with a resolution of 0.1 kPa. The samples were heated in the calorimeter from 93 K to 298 K at the rate 0.15 K min^{-1} to dissociate gas hydrate and the internal pressure, temperature, and

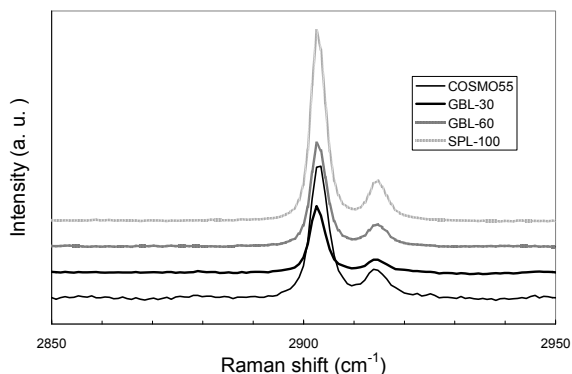


Figure 3. Raman spectra of C-H stretching mode of methane hydrate in glass beads.

heat flow to/from the sample were recorded.

2.3. Powder X-ray diffraction measurement

Powder X-ray diffraction (PXRD) measurements were done in $2\theta/\theta$ step scan mode using CuK α radiation ($\lambda = 1.541 \text{ \AA}$) with a step width of 0.02° in the 2θ range of $22\text{--}28.52^\circ$ for 5 min in total scan time (40 kV, 40 mA; Rigaku model Ultima III). The hydrate samples were mounted on a PXRD sample holder made from Cu 0.50 mm in thickness under a nitrogen gas atmosphere kept below 100 K. Temperature dependent PXRD measurements from 123 K up to 273 K were made every 10 K. The measurements from 123 K up to 173 K were made in vacuum and above 173 K up to 273 K were made under a dry nitrogen gas atmosphere to prevent vapor condensation on the sample surface using a low-temperature chamber (Rigaku). The temperature was kept at a constant value with maximum 0.1 K temperature deviations during each PXRD measurement. The use of rather thin samples allowed us to control the sample temperature at specific values without any significant waiting time before each measurement.

3. RESULTS AND DISCUSSION

3.1. Cage occupancy of methane hydrate in porous media

The Raman spectra of methane hydrate samples formed in glass beads are shown in Fig. 3. These signals have two peaks at $2902.9 \pm 0.1 \text{ cm}^{-1}$ and $2914.6 \pm 0.1 \text{ cm}^{-1}$, representing the methane molecule encaged in large and small cages, respectively. For

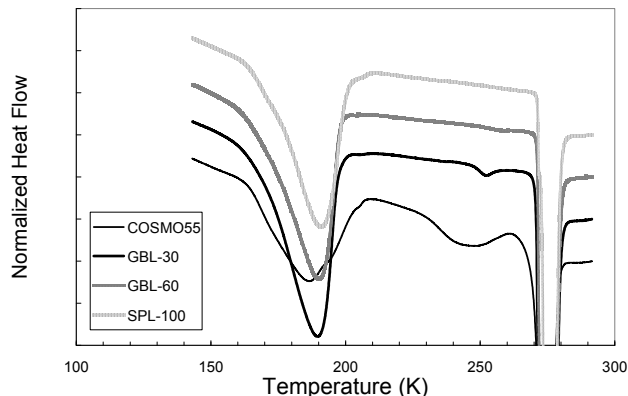


Figure 4. Thermograph shows the changes of heat flow. Negative direction of the normalized heat flow means endothermic.

all samples, the cage occupancies of large and small cage are calculated as 0.976 ± 0.001 and 0.831 ± 0.030 , respectively, and the hydration number was estimated to be 6.12 ± 0.04 . These results indicate that their cage occupancy and hydration number agree well with those of bulk methane hydrate reported by the previous works^{17,21} and the grain size of glass beads ranged from 0.4 to 100 μm seems to be not effective parameter to them.

3.2. Dissociation process of methane hydrate with glass beads

3.2.1. Calorimetric measurement

The thermographs of the sample are shown in Fig. 4. The primary negative peak appeared from 150 K to 200 K corresponds to the dissociation of methane hydrate. The other peak appeared from 270 K to 280 K is due to ice melting. The thermograph of SPL-100 (large grain size, 100 μm) seemed to be almost same as that of fine particles of methane hydrate in the previous work¹⁸. On the other hand, negative peaks of the secondary stage appeared in the case of COSMO55 and GBL-30. Because these peaks are endothermic and the internal pressures of the cell increased simultaneously, they are a part of unusual dissociation of methane hydrate.

In the process of methane hydrate dissociation, inner pressure increased with temperature and reached to 0.054–0.060 MPa. Residual ratio of methane hydrate in the sample can be calculated from the time variation of inner pressure (Fig. 5) by assuming that all the methane hydrate survived was dissociated at 273.2 K. The most part of the samples of GBL-30,

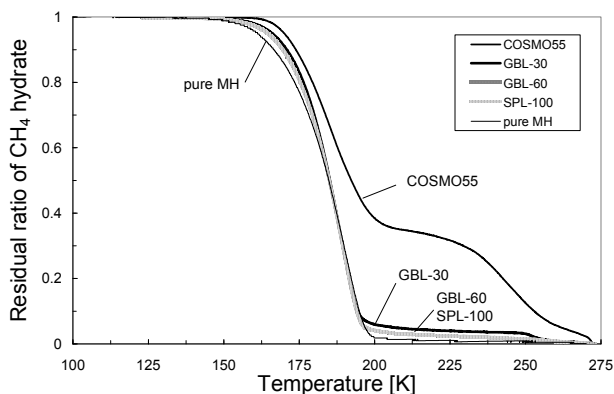


Figure 5. Residual ratio of methane hydrate in the sample plotted against temperature. GBL-60 is overlapped with SPL-100.

GBL-60, and SPL-100 dissociated from 150 K to 200 K as well as pure methane hydrate. The dissociation curves of GBL-60 and SPL-100 are similar to that of pure methane hydrates with no glass beads¹⁸, though the GBL-30 sample slightly remained up to around 250 K. On the other hand, in the case of fine particle (COSMO55) about 40% of the hydrate still remained at 200 K, although the primary stage (150-200 K) is the same as other samples corresponding to the dissociation temperature of methane hydrate. The secondary stage of COSMO55 sample started from 210 K and the dissociation progressed slowly up to the melting point of ice. In this stage, the increase of dissociation speed just below 273 K, as reported by Handa³ due to large hydrate crystals, was not observed. This result is consistent with the fact that the COSMO55 sample contained only small hydrate crystals.

3.2.2. Powder X-ray diffraction measurement

Fig. 6 shows the PXRD profiles for the methane hydrate dissociation process on going from structure I hydrate (sl) to ice as the temperature increased from 123 to 273 K in steps of 10 K with a 2θ -scan time of 5 min. Several diffraction peaks assigned to ice become evident at around 163 K, and the peak intensities increase with temperature while the methane hydrate diffraction peak intensities decrease. This indicates that the dissociated methane hydrate transformed into ice.

The relative volume ratios for various hydrates were measured by PXRD and were analyzed as a function of temperature (Fig. 7). The samples of SPL-100, GBL-60, and GBL-30 dissociated quickly, whereas more than 60 % of COSMO55 still remained at 200

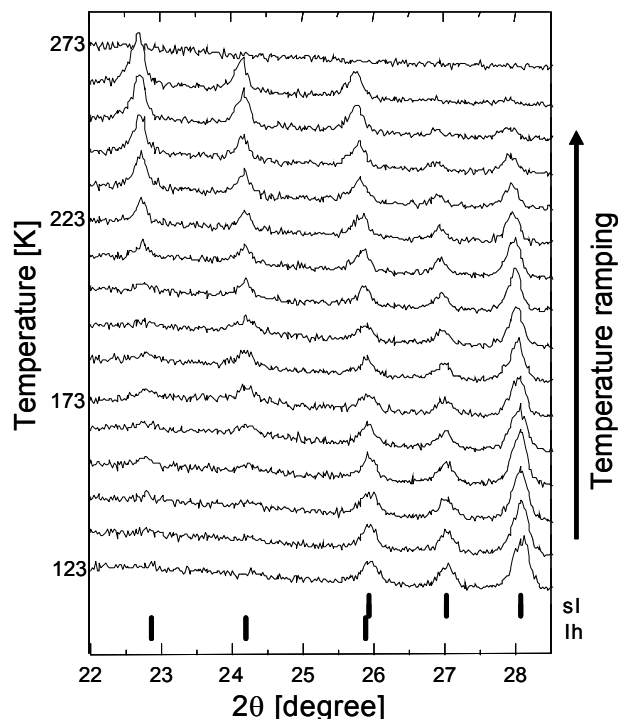


Figure 6. PXRD profiles in the dissociation process for the methane hydrate sample of COSMO55. The upper tick marks represent the peak positions for the structure I hydrate, and the lower represent hexagonal ice Ih.

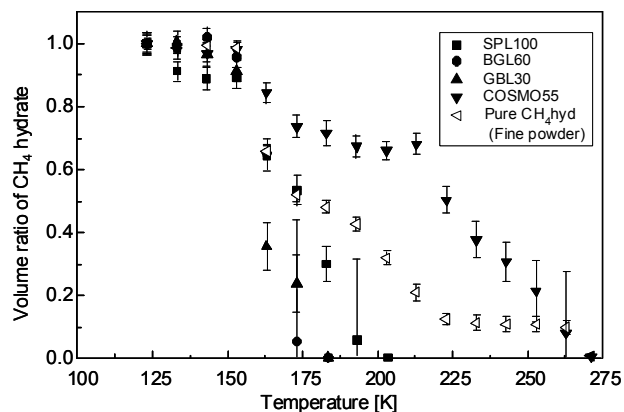


Figure 7. Volume ratio of methane hydrate in the sample by using PXRD data plotted against temperature.

K. The sample of COSMO55 stopped to dissociate around 200 K and the secondary stage of dissociation started from 220 K. These results by PXRD agree fairly well with those by the calorimeter (Fig. 5). The difference of residual ratio between the calorimetry and the PXRD at the same temperature was due to the difference of

temperature-controlling method and/or amount of sample for each measurement.

3.3. Grain size effect of glass beads on dissociation of methane hydrate with glass beads

The effect of grain size of methane hydrate on its dissociation process has been already reported¹⁵ that the dissociation rate of larger hydrate particles was lower than that of smaller particles. When methane hydrate forms in smaller pores constructed of fine glass beads, the size of hydrate becomes small and it seems easy to dissociate according to the grain size effect based on the gas diffusion model through ice layer for methane hydrate¹³. However, the results of our experiment (Figs. 5 and 7) are contrasting with those of the previous work¹⁵. In this study, methane hydrates in larger pore size (several tenth μm to 100 μm) quickly dissociated, and that in smaller pore size (0.4 μm) retained themselves and showed the secondary stage of dissociation. These results indicate that methane hydrate in coarse glass beads widely dispersed in the porous media could dissociate faster because the methane gas coming out from the dissociating hydrate likely escape through it easier than in fine glass beads.

Formation of supercooled water due to methane hydrate dissociation, as is suggested in the earlier experimental study²², could be on possible reason for plugging escape route of the gas. Distribution of unreacted water within porous media and effect of its freezing to hydrate dissociation remains unsettled questions. Inhomogeneity of grain size of hydrate particles due to fine glass beads also may affect to dissociation processes. We consider these subjects future investigation. In the next step of this study, we need to perform experiments with the range of critical size (submicron to several microns) of glass beads for further understanding of methane hydrate dissociation in porous media.

4. SUMMARY

We studied the dissociation process of methane hydrate formed with different size of glass beads by using the calorimeter. The hydrate within glass beads of submicron size tended to show self-preservation phenomena, while the hydrate within those of several tenths to 100 μm sizes dissociated rather quickly like fine particles of methane hydrate in the previous works¹⁵. It seems

reasonable to conclude that the effect of grain size of glass beads on the dissociation of hydrate is contrasting to that of grain size of hydrate particles. We propose our preliminary explanation for hydrate dissociation within glass beads taking into account our measurements.

ACKNOWLEDGMENTS

We thank to Dr. H. Ito of Kitami Institute of Technology (KIT) for particle size analysis of glass beads. We also thank to Mr. K. Mitsuhashi of KIT for FE-SEM images of glass beads. This research was supported by JSPS and RFBR under the Japan - Russia Research Cooperative Program.

REFERENCES

- (1) E.D. Sloan, Jr., *Nature*, **426**, 353-363 (2003).
- (2) Y.F. Makogon, S.A. Holditch, T.Y. Makogon, *J. Pet. Sci. Eng.*, **56**, 14-31 (2007).
- (3) Y.P. Handa, *J. Chem. Thermodyn.*, **18**, 891-902 (1986).
- (4) A. Hallbrucker, E. Mayer, *J. Chem. Soc. Faraday Trans.*, **86**, 3785-3792 (1990).
- (5) E.D. Ershov and V.S. Yakushev, *Cold Reg. Sci. Technol.*, **20**, 147-156 (1992).
- (6) V.S. Yakushev, V.A. Istomin, Gas-hydrate self-preservation effect, in: N. Maeno, T. Hondoh (Eds.), *Physics and Chemistry of Ice*, Hokkaido University Press, Sapporo, 1992, p.136-139.
- (7) L.A. Stern, S. Circone, S.H. Kirby, W.B. Durham, *J. Phys. Chem. B*, **105**, 1756-1762 (2001).
- (8) T. Komai, S.-P. Kang, J.-H. Yoon, Y. Yamamoto, T. Kawamura, M. Ohtake, *J. Phys. Chem. B*, **108**, 8062-8068 (2004).
- (9) W. Shimada, S. Takeya, Y. Kamata, T. Uchida, J. Nagao, T. Ebinuma, H. Narita, *J. Phys. Chem. B*, **109**, 5802-5807 (2005).
- (10) V.P. Melnikov, A.N. Nesterov, A.M. Reshetnikov, A.G. Zavodovsky, *Chem. Eng. Sci.*, **64**, 1160-1166 (2009).
- (11) S. Takeya, J.A. Ripmeester, *ChemPhysChem*, **11**, 70-73 (2010).
- (12) E.M. Chuvilin, O.M. Guryeva, Proc. 9th Int. Conf. on Permafrost, Fairbanks, Alaska, June 29 - July 3, 2008, p.263-267.
- (13) S. Takeya, W. Shimada, T. Uchida, J. Nagao, R.

- Ohmura, Y. Kamata, T. Ebinuma, H. Narita, *J. Phys. Chem. B*, **105**, 1756-1762 (2001).
- (14) W.F. Kuhs, G. Genov, D.K. Staykova, T. Hansen, *Phys. Chem. Chem. Phys.*, 4917-4920 (2004).
- (15) S. Takeya, T. Uchida, J. Nagao, R. Ohmura, W. Shimada, Y. Kamata, T. Ebinuma, H. Narita, *Chem. Eng. Sci.*, **60**, 1383-1387 (2005).
- (16) J.H. van der Waals, J.C. Platteeuw, *Adv. Chem. Phys.*, **2**, 1-57 (1959).
- (17) A.K. Sum, R.C. Burruss, E.D. Sloan, Jr., *J. Phys. Chem. B*, **101**, 7371-7377 (1997).
- (18) A. Hachikubo, T. Watanabe, K. Hyakutake, K. Abe, H. Shoji, Proc. 5th Int. Conf. on Gas Hydrates, Trondheim, Norway, June 13-16, 2005, p.1508-1511.
- (19) A. Hachikubo, R. Nakagawa, D. Kubota, H. Sakagami, N. Takahashi, H. Shoji, Proc. 6th Int. Conf. on Gas Hydrates, Vancouver, Canada, July 6-10, 2008, <http://hdl.handle.net/2429/2694>.
- (20) A. Hachikubo, M. Kida, M. Okuda, H. Sakagami, H. Shoji, *Seppyō*, **71**, 341-351 (2009) (in Japanese with English summary).
- (21) T. Uchida, T. Hirano, T. Ebinuma, H. Narita, K. Gohara, S. Mae, R. Matsumoto, *AIChE J.*, **45**, 2641-2645 (1999).
- (22) V.P. Melnikov, A.N. Nesterov, A.M. Reshetnikov, V.A. Istomin, V.G. Kwon, *Chem. Eng. Sci.*, **65**, 906-914 (2010).